ACS APPLIED MATERIALS & INTERFACES

Research Article

www.acsami.org

Superhydrophilic Multilayer Silica Nanoparticle Networks on a Polymer Microchannel Using a Spray Layer-by-Layer Nanoassembly Method

Kang Kug Lee* and Chong H. Ahn

Microsystems and BioMEMS Laboratory, School of Electronics and Computing Systems, University of Cincinnati, Cincinnati, Ohio 45221, United States

Supporting Information

ABSTRACT: Nanoporous and superhydrophilic multilayer silica nanoparticle networks have been developed on a hydrophobic cyclic olefin copolymer (COC) microchannel using a spray layer-by-layer (LbL) electrostatic nanoassembly method. This powerful and promising LbL method provides a simple, cost-effective, and high-throughput nanoporous silica multilayer selectively onto the hydrophobic polymer surfaces. These newly developed multilayer networks have also been successfully characterized by contact angle measurement, environmental scanning electron microscopy (ESEM), energy-dispersive X-ray spectroscopy (EDS), and atomic force microscopy (AFM). The superhydrophilic effect, which was confirmed by the contact angle measurements, of the silica networks ensured the hydrophilic nature of the selectively constructed nanoporous silica nanoparticles onto the patterned hydrophobic COC microchannel. The capillary effect of the developed surface was characterized by measuring the length of a test liquid driven by the induced capillary forces in an on-chip capillary pumping platform with horizontal microchannels. The pumping capability achieved from the sprayed nanoporous surface for the on-chip micropump was mainly due to the strong capillary imbibition driven by the multicoated bilayers of hydrophilic silica nanoparticles. The developed networks with spray-assembled nanoparticles were also applied for an on-chip blood plasma separation platform with closed microchannels. The spray LbL method developed in this work can be a highly practical approach for the modification of various polymer microchannels because of several advantages such as an extremely simple process for the multilayer formation and flexibly controlled surface functionality at room temperature.

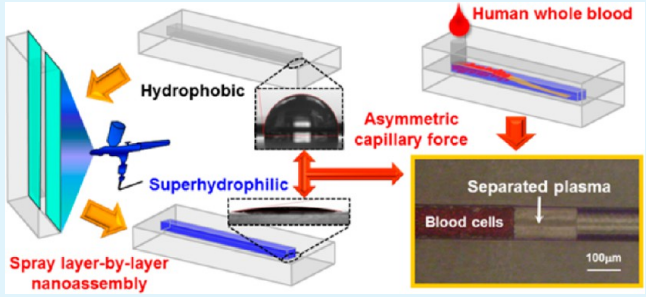

KEYWORDS: *spray layer-by-layer nanoassembly, superhydrophilic silica nanoparticle networks, capillary imbibition, cyclic olefin copolymer, asymmetric capillary force*

INTRODUCTION

Lab-on-a-chip (LOC), especially microfluidics-based LOC, technology has been considered a promising platform for a lot of applications over the past decades.[1−4] The most important aspect in microfluidic LOC devices is definitely handling and transport of fluids. Flow control of biological samples or reagents using a capillary force through a microchannel has been considered as one of the most attractive methods for the on-chip microfluidic devices of biological sensing or diagnostic systems toward point-of-care clinical testing (POCT).[5,6] Specifically, superhydrophilic wetting properties have significant effects on liquid behavior in the surface control applications such as capillary micropump or separator.[7−10] Therefore, the control of surface energy over the microchannel walls is very desirable for enhancing the wetting properties of microchannel surfaces.

Polymer-based microfluidic LOC devices are an alternative to those fabricated from glass and silicon substrates along with the standard lithographic microfabrication technology.[11] Polymers are suitable for single-use disposable devices since they offer low cost, good biocompatibility, and mass manufacture using high-throughput microfabrication techniques such as hot embossing or injection molding. Various polymer materials[12−18] such as polycarbonate (PC), polyvinyl chloride (PVC), polymethylmethacrylate (PMMA), polystyrene (PS), and COC have been used for the microfluidic LOC devices. Among them, a thermoplastic COC is of particular interest due to its combination of excellent UV transparency, low autofluorescence, low oxygen permeability, high mechanical strength, and compatibility with a broad range of chemicals and solvents.[19] However, COC has a hydrophobic nature, which possibly causes a low signal-to-noise ratio (S/N) due to the preference of molecular immobilization over the moderate hydrophobic surface. To improve the S/N, it is necessary to

Received: May 22, 2013
Accepted: August 5, 2013
Published: August 5, 2013

modify or functionalize the walls of the COC microchannels. Various techniques of polymer surface modification have been developed and reported in several reviews.[20−24] However, most of these procedures are not suitable for microfluidic devices because they rarely allow selective patterning on the surface of the microchannel. Furthermore, they usually require additional special instruments and harsh processing conditions. Thus, there is still a large demand for the development of a new technique for attaining highly hydrophilic surfaces on the patterned polymer microchannels for the better control of nonspecific binding in the microchannels as well as for attaining a strong capillary force to drive the liquids.

In this work, nanoporous superhydrophilic multilayer silica nanoparticle networks were fabricated onto a hydrophobic COC microchannel using a spray LbL electrostatic nanoassembly method (Scheme 1). This method is powerful yet facile, practical, easy-to-use (nontrained personnel), and high-throughput. The major advantage of this method is a dramatically reduced processing time needed for the multilayer formation, specifically, on the thermoplastic COC at room temperature. Surface functionality can be easily controlled by choosing appropriate polyelectrolytes. The coating method developed in this research is suitable for modifying the COC polymer microchannels over the existing methods.[24−27] More hydrophilic surface was successfully obtained in this LbL nanoassembly method (<10°) compared with the other methods such as O_2 plasma treatment (18−29.7°)[24,25] or photografting-induced modifications (20−46°).[26,27] The surface modified by O_2 plasma treatment is degraded over time and gradually returned to its original hydrophobic state.[25] After plasma treatment, the contact angle on COC recovered from 29° to below 40° for 24 h and reached 51° after 168 h. Since thermal bonding of the COC reduced its hydrophilicity, the modified surface can be affected by the processing conditions (120 °C, 10 MPa).[24] The surface modified by photografting can also be affected by the processing conditions for device fabrication[24] because the heating and aging conditions (50 °C for 1 h, 15 days)[27] were relatively low compared with the conditions in this research. This indicates that a lower contact angle and robust surface is preserved longer on the COC modified by spray LbL nanoassembly method. The pumping capability of the on-chip micropump was achieved from the strong hydrophilic properties of the nanoporous multicoated bilayers of sprayed silica nanoparticles. The asymmetric capillary force induced between nanoporous superhydrophilic surfaces and the uncoated hydrophobic COC surface offered a strong driving force for separating the blood plasma from the human whole blood. This property was mainly due to the nanoporous infiltration multilayer structures onto the COC microchannels.

Scheme 1. Schematic Diagram Showing Nanoporous Superhydrophilic Multilayer Silica Nanoparticle Networks Developed onto the Hydrophobic COC Microchannel Using a Spray LbL Electrostatic Nanoassembly Method

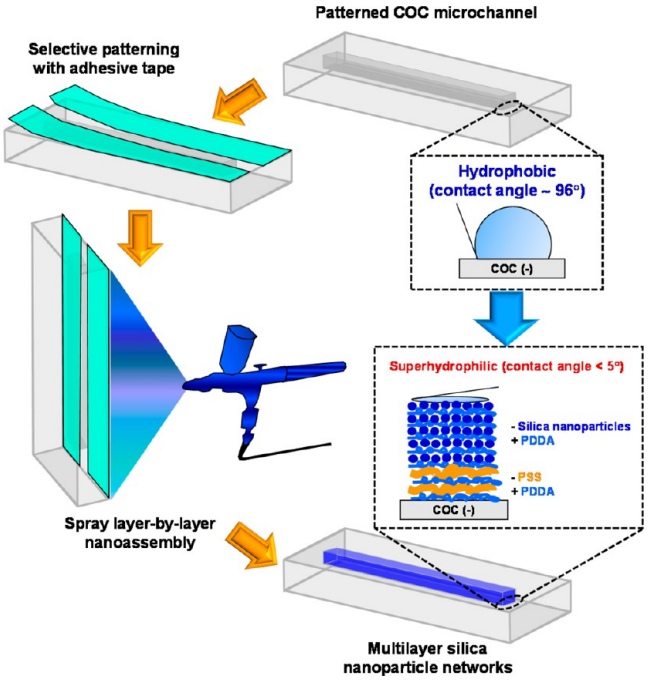

EXPERIMENTAL SECTION

2.1. Materials. Two kinds of polyelectrolyte, polydimethyldiallylammonium chloride (PDDA) and polysodium 4-styrenesulfonate (PSS), as an adhesion promoter were purchased from Sigma-Aldrich (St. Louis, MO). As hydrophilic nanoparticles with different sizes, SM-30 colloidal silica 30 wt % (7 nm diameter silica particles), Ludox HS-40 colloidal silica 40 wt % (12 nm diameter silica particles), and Ludox TM-40 colloidal silica 40 wt % (22 nm diameter silica particles) were also purchased from Sigma-Aldrich. In addition, the other silica nanoparticles (5% aqueous dispersion, 50 and 100 nm diameter silica particles) used for the nanoassembly were obtained from Polysciences (Warrington, PA). All negatively charged colloidal silica nanoparticles were diluted to 0.3 wt % in deionized (DI) water (18.2 MΩ cm). Polyelectrolyte solutions (PDDA and PSS) were diluted to 0.01 M in DI water. COC (TOPAS Advanced Polymers Inc., KY) was prepared to fabricate the microfluidic capillary pump. A blank bare COC wafer was cut into 15 mm × 15 mm rectangular shapes for the experiment. All rectangular COCs were cleaned by immersion in methanol and acetone solutions followed by a rinsing in deionized water and dried with high-pressure, high-purity nitrogen gas.

2.2. Spray Layer-by-Layer Nanoassembly Method. Figure 1 shows a schematic diagram of a typical multilayer buildup process by a spray LbL nanoassembly method.[28−30] The polyion solutions and rinsing solutions were supplied by enforced spraying in this process. The surface was modified by successive spraying of polyelectrolytes (PDDA or PSS or colloidal silica nanoparticles) on the COC microchannel surfaces, which were already activated by oxygen plasma (MARCH CS-1701 RIE, March Instruments Inc., CA) shown in Figure 1(a). The rest of the COC surface except the straight microchannel was covered with adhesive tape to avoid the surface from coating. In microfluidic chips with a complex microchannel, the whole surface of the chip can be covered with adhesive tape, and the covered surface with complex microchannel is simply engraved with a laser beam (Universal Laser Systems, Scottsdale, AZ). Accurately and quickly the laser beam engraves the covered surface following the designed complex microchannel without removing COC polymer or impacting surface integrity. This direct write laser method is feasible for microchips with a complex microchannel compared with the method by a conventional photographic method because it is a fast, environmentally "green", maskless, and single step process. To assemble multilayer networks, the treated COC substrates were placed vertically 20 cm from the spray nozzles. PDDA solution was spray deposited for 3 s and drained for 27 s as described in Figure 1(b). Then, rinsewater was sprayed for 20 s followed by 10 s of draining, so the total processing time of one polyelectrolyte layer is only 60 s which was a dramatically reduced processing time needed for the multilayer formation at room temperature. Spray rinsing was suspended, but drainage and evaporation of water continued. Alternate spraying deposition of oppositely charged polyions was performed onto the spray-rinsed surface and produced polyelectrolyte multilayer

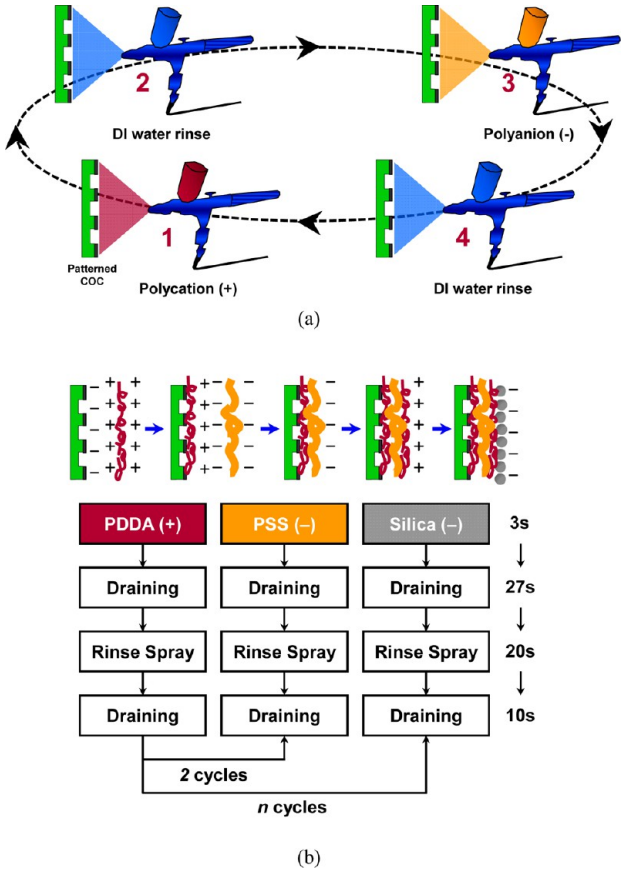

Figure 1. Nanoassembly protocol for (a) the deposition of polyelectrolyte multilayer films on patterned COC microchannels by spray LbL, where n is the number of bilayers; (b) spraying times and polyelectrolyte concentrations were based on the previous work,[28] and no drying step was performed between layer depositions.

film networks. The assembly of adhesion layer $[PDDA/PSS]_2$ and $[PDDA/SiO_2]_n$ networks was successfully implemented as displayed in Figure 1(b). By simply choosing suitable polyelectrolytes in the spray LbL nanoassembly, the surface functionality was easily organized as desired. After the spray LbL nanoassembly process, all samples were dried in an oven at 40 °C for 30 min (N_2 atmosphere). After the drying, they were put into the Fume hood under ultraviolet (UV) light to prevent the adsorption of molecules and contamination for further usage of the devices.

2.3. Design and Fabrication of the Testing Platforms. A computer numerical control (CNC) milling machine (Microlution 5100-S, Microlution Inc., IL) was selected as a method for fabricating a master mold. The CNC milling would manufacture various sizes of structures from micrometer-scale to millimeter-scale with high precision and high reliability. Three main steps for the CNC milling were computer-aided design (CAD), computer-aided manufacturing (CAM) programs, and a CNC machine for production. In this work, the straight microchannels with the dimension of 200 and 400 μm width × 100 μm depth × 47 mm length were designed by the AutoCAD (Autodesk Inc., CA) program. With a solid model in the Mastercam (CNC Software Inc., CT) CAM program, the two-dimensional CAD drawing would be converted to a three-dimensional drawing. Then, the tool paths were produced based on the three-dimensional structural information on the solid model. The created tool paths were converted to specific computer codes that were recognized by the Microlution 5100-S CNC machine and the CNC machine followed exactly as the codes for the actual device fabrication. After the whole procedures of CNC milling, the master mold containing straight microchannels was fabricated on the 6061 aluminum alloy which was 4 in. wide, 4 in. long, and 0.25 in. thick for the replica of COC microchannels. Then, COC substrates were patterned with microfluidic channels using a hot embossing technique for the spray LbL process. The spray LbL nanoassembly process with silica nanoparticles was followed by the surface modification of the patterned COC microchannel as described in Figure 1. Careful treatments in the cleanroom were required for modifying the COC surfaces by the spray LbL nanoassembly method. By simply choosing suitable polyelectrolytes in the spray LbL nanoassembly, the surface functionality was easily organized as desired. After the spray LbL nanoassembly process, all samples were dried in an oven at 40 °C for 30 min (N_2 atmosphere). After the drying, the samples were transferred to the fume hood under ultraviolet (UV) light to prevent the adsorption of molecules and contamination of the devices. When the samples were used for measurements, they were taken out of the fume hood right before the measurements. So, it is said that there is no contamination for further usage of the devices. Finally, the polymer substrate with microchannels was bonded with a cover polymer substrate by a thermoplastic fusion bonding technique using an embossing machine (MTP-10, Tetrahedron Associates Inc., San Diego, CA).

2.4. Characterization Methods for the Nanoassembled Silica Films. The contact angle analysis is a simple but a very powerful method for measuring the changes of surfaces at the monolayer level. The wettability of the spray-coated silica films on COC was characterized in ambient air at room temperature using a contact angle goniometer based on the sessile drop method. The mean contact angles with high purity DI water were determined by averaging values measured at five different points on the sample surface. An amount of 3 μL of DI water was applied on the sample surfaces using a micropipet. The images of the COC microchannel and the film formed by silica nanoparticles were characterized by ESEM (XL-30, Philips-FEI Company, Holland). EDS analysis was performed over the microchannel area with and without the silica nanoparticles to confirm the spray-assembled silica nanoparticles. The AFM images were obtained by Veeco Dimension 3100 AFM (Digital Instruments Inc., Santa Barbara, CA) under ambient conditions. Cantilevers with a spring constant of 0.03 N/m and silicon nitride tips were used. Several scans were performed over a given surface area. These scans were aimed at producing reproducible images to ascertain that there was no sample damage induced by the tip. Deflection and height mode images were scanned simultaneously at a fixed scan rate (between 2 and 4 Hz) with a resolution of 512 × 512 pixels.

2.5. Preparation of Human Whole Blood for On-Chip Blood Plasma Separator. A sample of whole human blood was procured from the department of Pathology and Laboratory Medicine at the University of Cincinnati. Among the sample blood contained in the BD Vacutainer Plus Plastic K_2EDTA Tube (Becton, Dickinson and Company, NJ), 3 μL of the whole blood was pipetted and dropped at the inlet of the blood plasma separator. Owing to the superhydrophilic nature of the modified surfaces in the separator, the blood flowed through the microchannel by induced strong capillary force without the application of external power. By using reference marks along with the microchannel, the movement of the separated plasma was monitored with an optical microscope.

RESULTS AND DISCUSSION

3.1. Surface Characterization with Contact Angle Measurements. Figure 2(a) shows that contact angles on the modified COC surfaces were measured as a function of five types of silica nanoparticles. The lowest contact angle with smallest standard deviation was obtained in 12 nm silica nanoparticles coated onto the COC surface. Therefore, the 12 nm silica nanoparticle was chosen for the spray LbL nanoassembly on the COC microchannels as the surface control applications such as microfluidic capillary pump or separator due to the strong hydrophilic nature of the multilayer nanoporous structure.

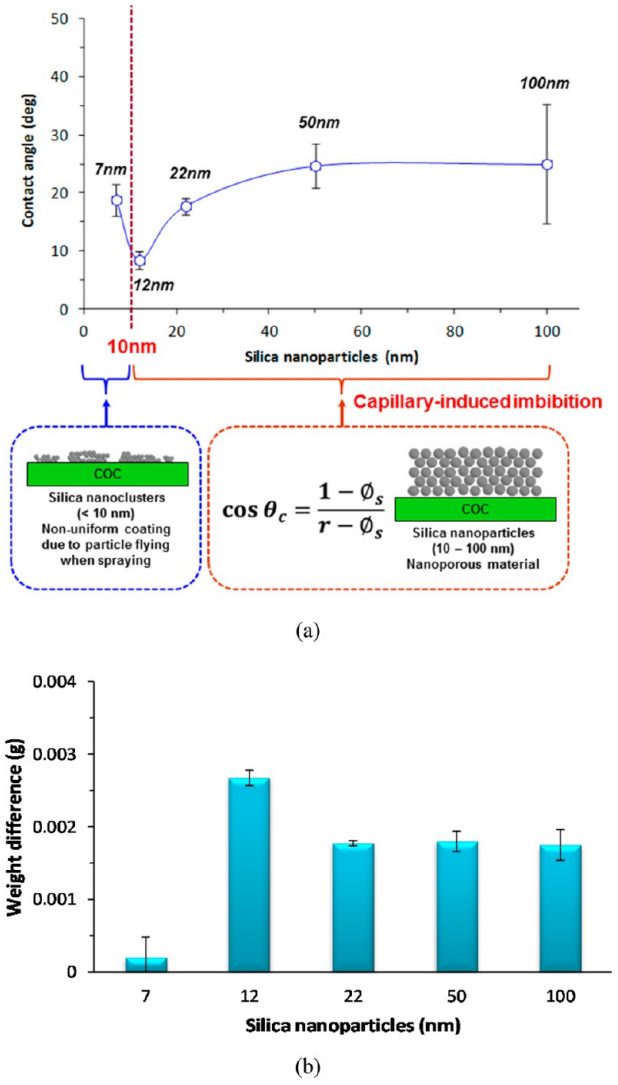

Figure 2. (a) Variation of contact angles on silica nanoparticle sizes with DI water droplets and (b) the weight difference between 1 bilayer and 5 bilayer coatings.

The contact angle variation with nanoparticle sizes was analyzed by *hemiwicking wetting*,[31,32] the dynamics of a droplet imbibing on a rough surface. A critical contact angle θ_c is defined as below

$$\theta < \theta_c, \quad \text{with } \cos\theta_c = \frac{1-\phi_s}{r-\phi_s} \tag{1}$$

The roughness factor r is the ratio of the actual surface area over the projected one, and ϕ_s is the solid fraction of the projected area covered by the top of the roughness. For the porous materials, the liquid can be infiltrated between hollows induced by the capillary force, so the solid can be regarded as textured structures. While a liquid droplet is placed on the rough surface satisfying $\theta < \theta_c$ in eq 1, infiltration of the liquid into the hollows of the rough surface is energetically favorable. Equation 1 exhibits the intermediate condition between for spreading and for imbibition. In other words, the condition generally states a critical contact angle intermediate between 0 and $\pi/2$ if the $r > 1$ and $\phi_s < 1$. Spreading on a surface occurs if $\theta_c \to 0$ for a flat surface ($r \to 1$); however, the classical condition for capillary rise is satisfied when $\theta_c \to \pi/2$ in porous media ($r \to \infty$). On the basis of the dynamics of capillary imbibition, a smaller contact angle was obtained in the smaller silica nanoparticles deposited on COC compared with the larger silica nanoparticles on COC. Below the 10 nm scale, however, this *hemiwicking wetting* cannot be properly applied because the nanoparticles are not simply assembled onto the COC surface. For the size between 1 and 10 nm with a narrow size distribution, the nanostructures can be classified into nanoclusters.[33] Nanosized particles are usually flying away from the targeted substrates during spraying because their kinetic energy is sufficiently high. The amount of free flying particles was especially high in relatively smaller nanoparticles (1−10 nm) considering the weight difference between bilayers in Figure 2(b). It is noted that the weight difference between the bilayers in 7 nm was dramatically low, which presents a low deposition ratio compared with that in 12 or 22 nm. The water contact angle of the surface assembled with silica nanoclusters of 7 nm was relatively high at about 18° compared with that of 12 nm. Therefore, the minimum contact angle value in 12 nm silica nanoparticles was attributed to the dynamics of a capillary imbibition on LbL assembled nanoporous architectures as well as the safely assembled nanoparticles onto the COC surface.

Figure 3 shows the changes in contact angle for a first water drop (3 μL) as a function of time.[34] The contact angles of all

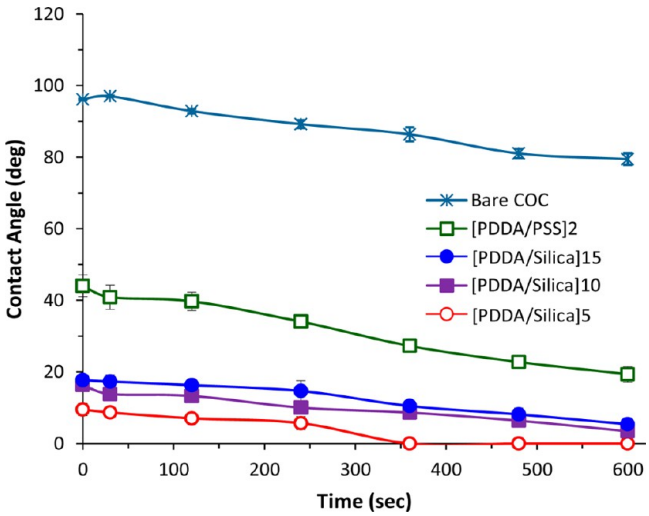

Figure 3. Contact angle variations as a function of time in a different number of silica bilayers on COC surfaces.[34]

surfaces were gradually decreased over time. Highly wettable surfaces were obtained with coatings of 5, 10, and 15 bilayers, but superhydrophilic behavior was only achieved in coating of five bilayers for the film that completely wets (contact angle below 5° compared to bare COC with a contact angle of 90°) with DI water after 250 s. This dramatic drop in contact angles indicated that the COC surface would be superhydrophilic with silica nanoparticles due to the intrinsically high level of wettability of the silica nanoparticles coupled with the nanoporous nature of the multilayer surface. Thus, the coating of five [PDDA/silica] bilayers was chosen as an optimum coating of bilayers to obtain the maximum nanoporous capillary pumping effect in this process.

3.2. Surface Characterization with ESEM and EDS.

Nanoassembled silica film onto the COC microchannel and the uncoated COC microchannel were characterized by ESEM as shown in Figure 4. The high-resolution image of the silica

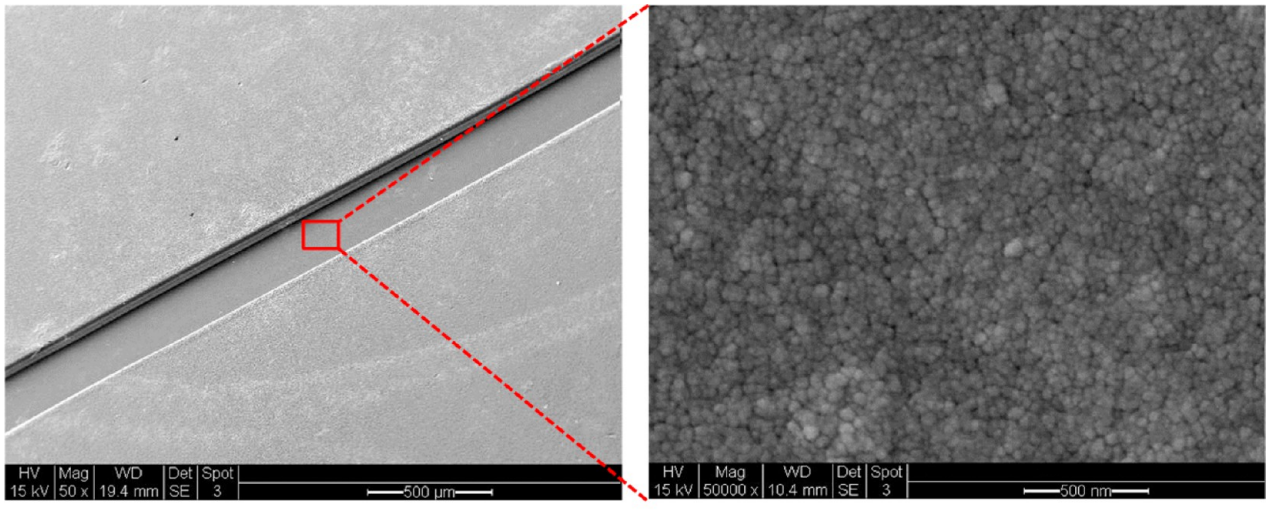

(a)

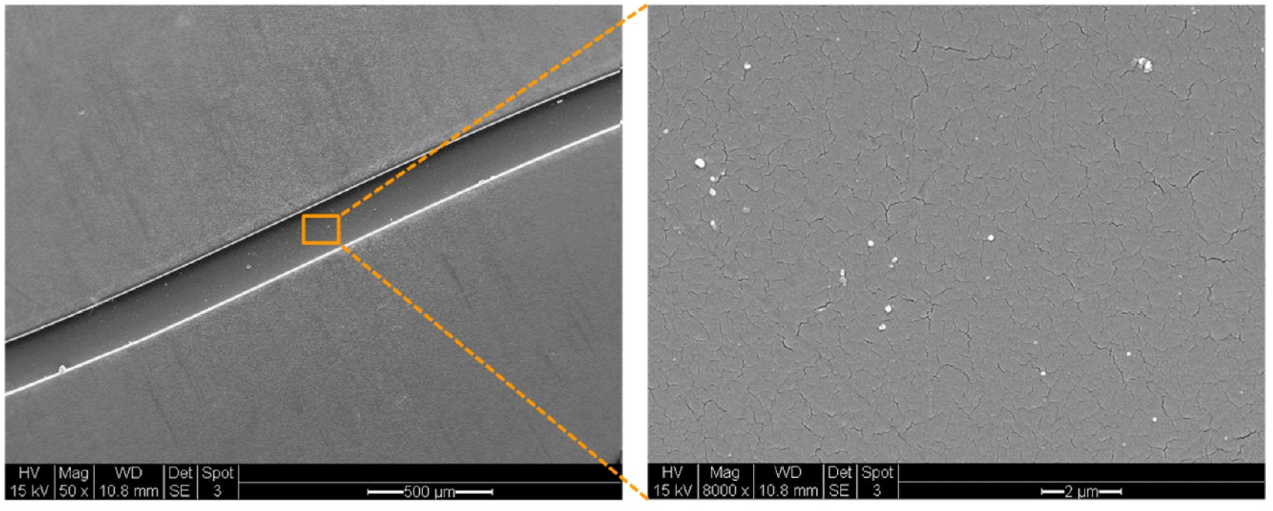

(b)

Figure 4. ESEM images of the (a) silica nanoparticle networks deposited onto the COC microchannel and (b) the bare COC microchannel.

nanoparticles onto the COC microchannel was depicted in Figure 4(a). This close and uniform nanostructure observed in the ESEM image enhanced the nanoporous capillary action of the deposited silica nanoparticles. The enhanced nanoporous capillary force was attributed to the hydrophilic nature of the nanoassembled silica nanoparticles on the hydrophobic COC surface as well as the imbibition into porous architecture. To confirm the assembled silica nanoparticles, EDS analysis was performed over the COC microchannel areas with and without the silica nanoparticles as shown in Figure 5. The chemical signature of silicon and oxygen peaks in EDS spectra was displayed within the COC microchannel area with the coated silica nanoparticles in Figure 5(a). These signatures clearly presented that the nanostructure of silica nanoparticles was successfully constructed onto the COC microchannel by the spray LbL nanoassembly method.

3.3. Surface Characterization with AFM. Figure 6 shows a model for AFM measurement, surface morphology, and roughness information of the spray nanoassembled silica networks obtained by AFM. The surface topography on the nanometer length scale was altered by simply varying the number of silica bilayers. Moreover, increasing the number of silica bilayers resulted in a corresponding increase in root-mean-square (RMS) roughness values. Five silica bilayers had smoother surfaces with a low RMS roughness of 4.83 nm in Figure 6(b), compared to fifteen silica bilayers, which had an RMS roughness of 12.1 nm in Figure 6(d). Thus, the surface roughness value was increasing with the number of silica bilayers assembled by the spray LbL nanoassembly method.

3.4. Long-Term Stability of the Spray Nanoassembled Silica Nanoparticles on COC. The long-term stability of the deposited films is an important parameter for the evaluation of the film performance. The durability of the spray nano-assembled silica nanoparticles on the COC surface was investigated by monitoring the contact angle variations over 60 days in Figure 7. The coated samples were kept in outdoor exposure during the periods at room temperature. The results showed that superhydrophilic coating by the spray LbL

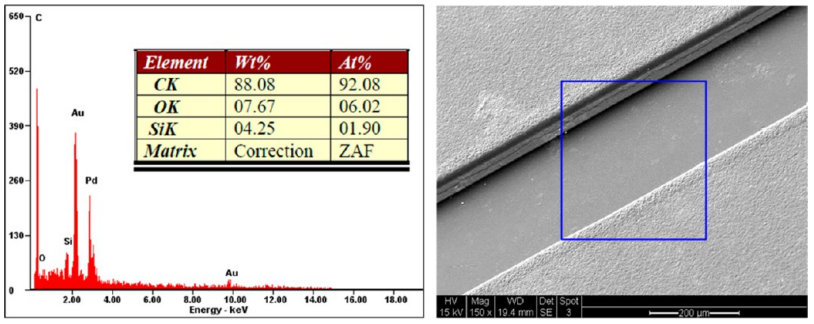

(a)

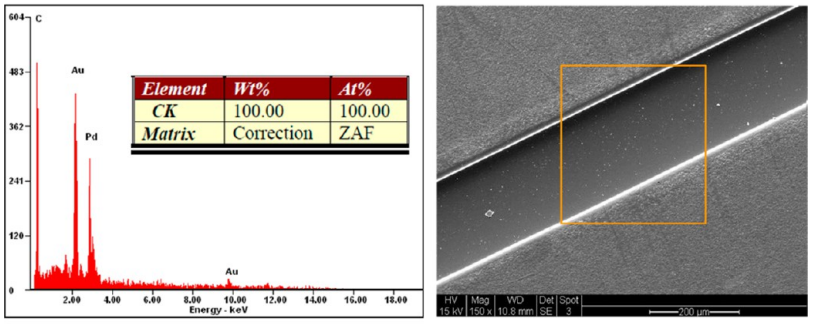

(b)

Figure 5. EDS spectra with elemental maps of the (a) silica nanoparticle networks deposited onto the COC microchannel and (b) the bare COC microchannel.

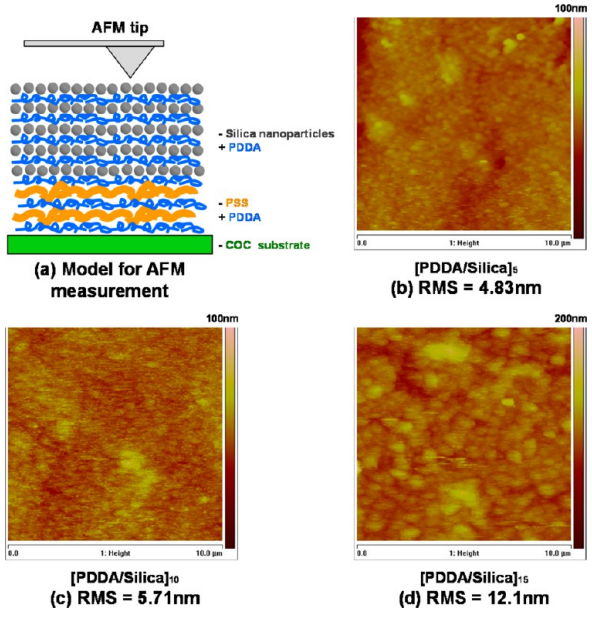

Figure 6. AFM measurements: (a) model for AFM measurement; (b), (c), and (d) AFM images and RMS values of the spray nanoassembled silica nanoparticles on COC surfaces as a function of silica bilayers.

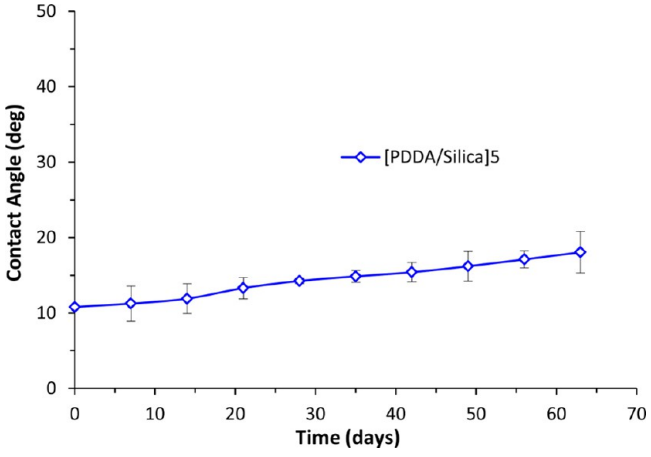

Figure 7. Long-term stability of the spray nanoassembled silica nanoparticle networks on the COC surface.

nanoassembly method was chemically stable over time. Contact angle measurements of five different types of silica multilayer networks on COC substrates have been performed to evaluate the robustness of the films shown in Figure S1 (Supporting Information). The contact angles of tapping coated samples and samples on a hot plate (120 °C, 30 min) were almost the same as those of spray nanoassembled samples. This result indicates that the modified surface is robust and stable in spite of the treated conditions. However, there were slight increases of the contact angles when the coated samples were dipped into the water for 30 min and the samples were mechanically separated from the thermally bonded device. These results show that the spray nanoassembled silica networks were safely deposited on the COC substrate even if the samples were under harsh environments. The measured contact angles in several harsh environments were fairly low compared with that of the bare COC surface in Figure S1 (Supporting Information). Therefore, it is noted that the nanoassembled silica networks were not easily removed from the COC even if the water or the biological fluids were applied onto the coated surfaces.

3.5. Flow Characterization in the Microfluidic Capillary Pump. Two types of microchannels 200 and 400 μm wide in horizontal platform were prepared to characterize the nanoporous capillary pumping effect. All microchannel surfaces were coated with five [PDDA/silica] bilayers. A droplet of 3 μL of red-colored food dye was injected into the inlet of the microchannel using a micropipet. A flow was produced through the microchannel to reach the outlet reservoir by autonomous capillary. As shown in Figure 8, the liquid front of the food dye

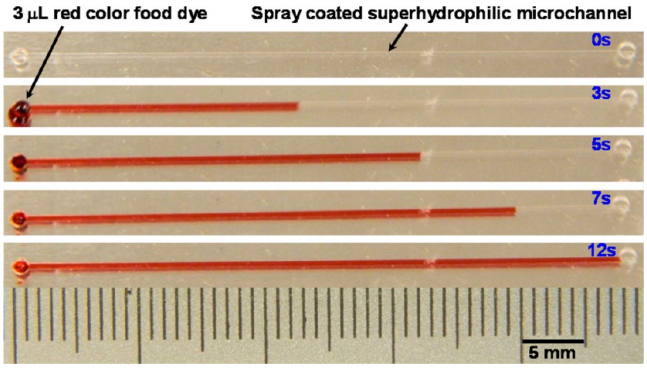

Figure 8. Flow characterization in an on-chip horizontal capillary pump with COC microchannels of 400 μm × 100 μm × 47 mm.

moved up to 47 mm without any additional forces within 12 s. It was found that the liquid moved quickly at the beginning time, and the speed of the movement slightly decreased with the succeeding time until the liquid reached the outlet reservoir. Figure 9 shows the relationship between the relative distance of

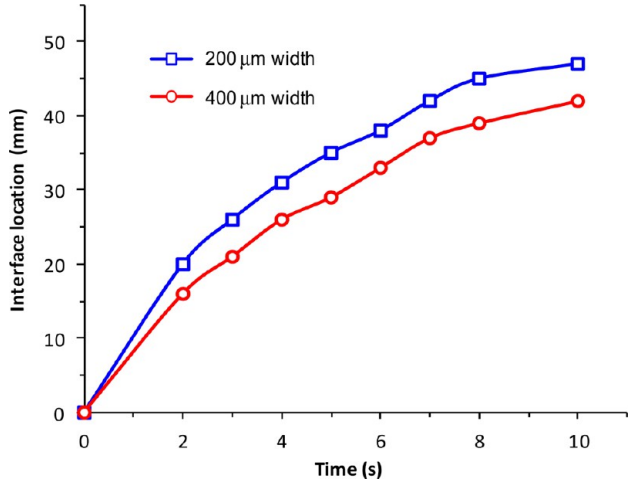

Figure 9. Characterization of pumping capability in an on-chip horizontal capillary pump with COC microchannels of 200 and 400 μm wide.

liquid–gas interface locations from inlet to outlet reservoirs and time. The liquid front location of the food dye moved approximately 42 mm for the initial seven seconds and moved 5 mm during the succeeding three seconds when the width of the microchannel was 200 μm. As the width is 400 μm, the liquid–gas interface location could only move 37 mm for the first seven seconds but moved 6 mm during the succeeding three seconds. Thus, the capillary pumping effect was decreasing with the increasing width of the microchannels.

3.6. On-Chip Blood Plasma Separation in a Closed COC Microchannel. Figure 10 displays the on-chip blood

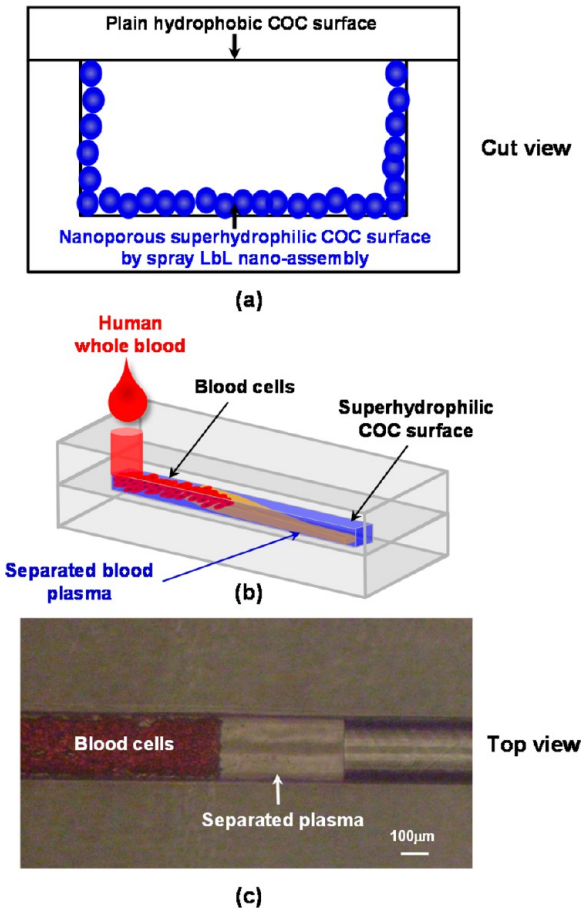

Figure 10. On-chip blood plasma separation using a horizontal capillary pump with a closed 200 μm wide COC microchannel: (a) coating strategy of sidewall coatings only; (b) blood plasma separator with a closed COC microchannel; (c) magnified view of the separated plasma.

plasma separation in a closed COC microchannel. The blood cells were not allowed to move forward because of the viscosity difference among the whole blood. However, the blood plasma was separated from the whole blood due to a strong asymmetric capillary force[34] developed between a plain hydrophobic COC surface and three nanoporous superhydrophilic surfaces although the microchannel was closed in the capillary pump shown in Figure 10(b). About 10 nL volume of the separated plasma was finally obtained in the blood plasma separator depicted in Figure 10(c). This platform is a good example of the passive on-chip capillary pump with nanoporous superhydrophilic silica multilayers onto a hydrophobic COC microchannel using a spray LbL electrostatic nanoassembly method. It is very desirable to generate a strong asymmetric capillary force among the surfaces for separating the blood plasma from whole blood in a closed microchannel.

CONCLUSION

In conclusion, nanocapillary-driven superhydrophilic multilayer networks with 12 nm silica nanoparticles onto the patterned COC microchannels were successfully prepared by a spray LbL nanoassembly method. The resulting multilayer networks were

successfully characterized by several characterization methods and two testing platforms. The result showed that the on-chip capillary micropump drove the food dye 47 mm long without any additional power within 12 s. The capillary pumping effect was decreasing with the increasing width of the microchannels. An additional platform with closed microchannels for on-chip blood plasma separation presented that about 10 nL volume of blood plasma was successfully separated from the whole blood. This separation result was due to the strong asymmetric capillary force developed between a plain hydrophobic COC surface and the three nanoporous superhydrophilic surfaces in spite of the closed microchannels in the platform. Therefore, the developed superhydrophilic silica multilayer networks using a spray LbL nanoassembly method can also be an ideal platform for capillary-driven lateral flow bioassays toward POCT.

■ ASSOCIATED CONTENT

Ⓢ Supporting Information

The robustness of the spray-assembled SiO_2 multilayers in several different conditions has been described. This material is available free of charge via the Internet at http://pubs.acs.org.

■ AUTHOR INFORMATION

Corresponding Author

*E-mail: leek8@mail.uc.edu.

Notes

The authors declare no competing financial interest.

■ ACKNOWLEDGMENTS

The authors gratefully would like to acknowledge the Transducer Research Foundation for support for the Student Travel Award Program. This work was partially supported by The Ohio Center for Microfluidic Innovation (OCMI) at University of Cincinnati. The authors would like to acknowledge Dr. Ha Won Kim and Dr. Motoi Okada in the Department of Pathology and Laboratory Medicine at the University of Cincinnati for procuring human whole blood samples. The authors are also thankful for valuable discussions and comments from Dr. Punit Boolchand, Dr. Fred R. Beyette, Dr. Ian Papautsky, Dr. Jason C. Heikenfeld, and Dr. Gregory Beaucage at University of Cincinnati.

■ REFERENCES

(1) Craighead, H. *Nature* **2006**, *442*, 387−393.
(2) Erickson, D.; Li, D. *Anal. Chim. Acta* **2004**, *507*, 11−26.
(3) El-Ali, J.; Sorger, P. K.; Jensen, K. F. *Nature* **2006**, *442*, 403−411.
(4) Sia, S. K.; Whitesides, G. M. *Electrophoresis* **2003**, *24*, 3563−3576.
(5) Henry, A. C.; Tutt, T. J.; Galloway, M.; Davidson, Y. Y.; McWhorter, C. S.; Soper, S. A.; McCarley, R. L. *Anal. Chem.* **2000**, *72*, 5331−5337.
(6) Kung, C. F.; Chiu, C. F.; Chen, C. F.; Chu, C. C. *Microfluid. Nanofluid.* **2009**, *6*, 693−697.
(7) Bulmus, V.; Ayhan, H.; Piskin, E. *Chem. Eng. J.* **1997**, *65*, 71−76.
(8) Walker, G. M.; Beebe, D. J. *Lab Chip* **2002**, *2*, 131−134.
(9) Zimmermann, M.; Schmid, H.; Hunziker, P.; Delamarche, E. *Lab Chip* **2007**, *7*, 119−125.
(10) Lynn, N. S.; Dandy, D. S. *Lab Chip* **2009**, *9*, 3422−3429.
(11) Burns, M. A.; Johnson, B. N.; Brahmasandra, S. N.; Handique, K.; Webster, J. R.; Krishnan, M.; Sammarco, T. S.; Man, P. M.; Jones, D.; Heldsinger, D.; Mastrangelo, C. H.; Burke, D. T. *Science* **1998**, *282*, 484−487.
(12) Becker, H.; Heim, U. *Sens. Actuators A* **2000**, *83*, 130−135.
(13) Klank, H.; Kutter, J. P.; Geschke, O. *Lab Chip* **2002**, *2*, 242−246.
(14) Khan Malek, C. G. *Anal. Bioanal. Chem.* **2006**, *385*, 1351−1361.
(15) Marchand, G.; Broyer, P.; Lanet, V.; Delattre, C.; Foucault, F.; Menou, L.; Calvas, B.; Roller, D.; Ginot, F.; Campagnolo, R.; Mallard, F. *Biomed. Microdevices* **2007**, *10*, 35−45.
(16) Huang, Y.; Liu, S.; Yang, W.; Yu, C. *Appl. Surf. Sci.* **2010**, *256*, 1675−1678.
(17) Suriano, R.; Kuznetsov, A.; Eaton, S. M.; Kiyan, R.; Cerullo, G.; Osellame, R.; Chichkov, B. N.; Levi, M.; Turri, S. *Appl. Surf. Sci.* **2011**, *257*, 6243−6250.
(18) Ogilvie, I. R. G.; Sieben, V. J.; Cortese, B.; Mowlem, M. C.; Morgan, H. *Lab Chip* **2011**, *11*, 2455−2459.
(19) Lamonte, R. R.; McNally, D. *Plast. Eng.* **2000**, *56*, 51−55.
(20) Belder, D.; Ludwig, M. *Electrophoresis* **2003**, *24*, 3595−3606.
(21) Makamba, H.; Kim, J. H.; Lim, K.; Park, N.; Hahn, J. H. *Electrophoresis* **2003**, *24*, 3607−3619.
(22) Dolnik, V. *Electrophoresis* **2004**, *25*, 3589−3601.
(23) Liu, K.; Lee, M. L. *Electrophoresis* **2006**, *27*, 3533−3546.
(24) Ahn, C. H.; Choi, J. W.; Beaucage, G.; Nevin, J. H.; Lee, J. B.; Puntambekar, A.; Lee, J. Y. *Proc. IEEE* **2004**, *92*, 154−173.
(25) Jeon, J. S.; Chung, S.; Kamm, R. D.; Charest, J. L. *Biomed. Microdevices* **2011**, *13*, 325−333.
(26) Stachowiak, T. B.; Mair, D. A.; Holden, T. G.; Lee, L. J.; Svec, F.; Frechet, J. M. J. *J. Sep. Sci.* **2007**, *30*, 1088−1093.
(27) Jena, R. K; Yue, C. Y. *Biomicrofluidics* **2012**, *6*, 012822−1−012822−12.
(28) Izquierdo, A.; Ono, S. S.; Voegel, J. C.; Schaaf, P.; Decher, G. *Langmuir* **2005**, *21*, 7558−7567.
(29) Schaaf, P.; Voegel, J.-C.; Jierry, L.; Boulmedais, F. *Adv. Mater.* **2012**, *24*, 1001−1016.
(30) Decher, G.; Schlenoff, J. B. *Multilayer Thin Films: Sequential Assembly of Nanocomposite Materials*, 2nd ed.; Wiley: New York, 2012.
(31) Bico, J.; Thiele, U.; Quere, D. *Colloids Surf., A: Physicochem. Eng. Asp.* **2002**, *206*, 41−46.
(32) Chandra, D.; Yang, S. *Langmuir* **2011**, *27*, 13401−13405.
(33) Fahlman, B. D. *Materials Chemistry*; Springer: New York, 2007.
(34) Lee, K. K.; Ahn, C. H. *Lab Chip* **2013**, *13*, 3261−3267.